Available online at www.sciencedirect.com
SCIENCE DIRECT®
Journal of Solid State Chemistry 177 (2004) 3757–3767
JOURNAL OF SOLID STATE CHEMISTRY
www.elsevier.com/locate/jssc

Synthesis, characterization and thermal properties of new aromatic quaternary ammonium bromides: precursors for ionic liquids and complexation studies

Sara Busi, Manu Lahtinen*, Jarmo Ropponen, Jussi Valkonen, Kari Rissanen

Department of Chemistry, University of Jyväskylä, P.O. Box 35, 40014 Jyväskylä, Finland

Received 25 February 2004; received in revised form 22 June 2004; accepted 24 June 2004
Available online 27 August 2004

Abstract

Series of new aromatic $R_2R'_2N^+Br^-$ (R = benzyl, 4-methylbenzyl, 2-phenylethyl, 3-phenylpropyl; R' = ethyl, methyl, isopropyl) or $RR'_2NH^+Br^-$-type (R = benzyl, R' = isopropyl) quaternary ammonium bromides were prepared by using novel synthetic route in which a formamide (*N*,*N*-diethylformamide, *N*,*N*-dimethylformamide, *N*,*N*-diisopropylformamide) is treated with aralkyl halide in presence of a weak base. The compounds were characterized by ^{1}H-NMR and ^{13}C-NMR spectroscopy and mass spectrometry. Structures of the crystalline compounds were determined by X-ray single crystal diffraction, and in addition the powder diffraction method was used to study the structural similarities between the single crystal and microcrystalline bulk material. Three of the compounds crystallized in monoclinic, two in orthorhombic and one in triclinic crystal system, showing ion pairs, which are interconnected by weak hydrogen bonds and weak $\pi-\pi$ interactions between the phenyl rings. Three of the compounds appeared as viscous oil or waxes. Finally, TG/DTA and DSC methods were used to analyze thermal properties of the prepared compounds. The lowest melting points were obtained for diethyldi-(2-phenylethyl)ammonium bromide (122.2 °C) and for diethyldi-(3-phenylpropyl)-ammonium bromide (109.1 °C). In general, decomposition of the compounds started at 170–190 °C without identifiable cleavages, thus liquid ranges of 30–70 °C were observed for some of the compounds.

Keywords: Quaternary ammonium bromide; Ionic liquid; X-ray single crystal diffraction; X-ray powder diffraction; Thermal analysis; Weak interactions

1. Introduction

Quaternary ammonium compounds have found significant use as surfactants [1–3] and phase-transfer catalysts [4–7]. They have been utilized in many applications as disinfectants, detergents, fungicides, bactericides and bleach activators [8–17]. Recently, ammonium compounds have found use in advanced battery technology [18–21] due to their ionic liquid [22–24] behavior and as a size probing guests in molecular encapsulation studies [25–28]. The synthetic methods for quaternary ammonium compounds have been known for a long time [29–35]. They can be prepared, for example, by reacting tertiary amines with various quaternizing agents [36–40], but substituted or unsubstituted alkyl halides are most used. The disadvantage of this synthetic method in some cases is the separation of the product from the potential side products and/or solvent at the end of the reaction. Furthermore, the purification of the product has been found difficult and costly, resulting in low yields. We have recently shown that using a novel one-pot synthesis, $R_4N^+X^-$, $R_2R'_2N^+X^-$ and $R_2R'R''N^+X^-$-type of quaternary ammonium halides can be provided selectively, as the product is easily separable with high purity from the reaction mixture [41].

*Corresponding author. Tel.: +358-14-260-2624; Fax: +358-14-260-2501.
E-mail address: makrla@cc.jyu.fi (M. Lahtinen).

0022-4596/$ - see front matter © 2004 Elsevier Inc. All rights reserved.
doi:10.1016/j.jssc.2004.06.046

In this paper we present the synthesis, structural characterization and thermal behavior of nine new aromatic quaternary ammonium bromides **1–9**. Structural characterizations in the solid state (compounds **1–5** and **8**) and in the liquid state (compounds **1–9**) are reported. The aim is to develop a family of new quaternary ammonium compounds and their derivatives to be used as ionic liquids and phase-transfer catalysts, and also as guests in molecular encapsulation studies. The applicability of the synthesized quaternary ammonium halides is to be extended by anion exchange to alter the chemical and physical properties (melting point, solubility, acidity, thermal stability, solvation strength) to those more suitable for ionic liquid applications. The recent developments in the research of the ionic liquids have shown their potential over conventional organic solvents in certain reaction processes [42–44] and/or as a catalyst in transition metal synthesis [45–47], in Friedel–Craft catalysis [48–50], and in various polymer processes [51–53]. Furthermore, the phase-transfer catalyst properties are to be exploited in further studies.

2. Experimental section

2.1. Synthesis: general procedure

Compounds **1–9** (Scheme 1) were prepared by using synthetic route described earlier [41] (procedure presented in Scheme 2). All chemicals used in the synthesis were commercially available and used as received from the manufacturer.

All reactants were placed in the reaction flask. The reaction mixture was stirred at chosen temperature for 48–72 h. After cooling down to RT, the mixture was filtered to remove excess carbonate and alkaline metal halide following with the evaporation of filtrate to minimum volume. The final extraction of product was performed with one of the following methods.

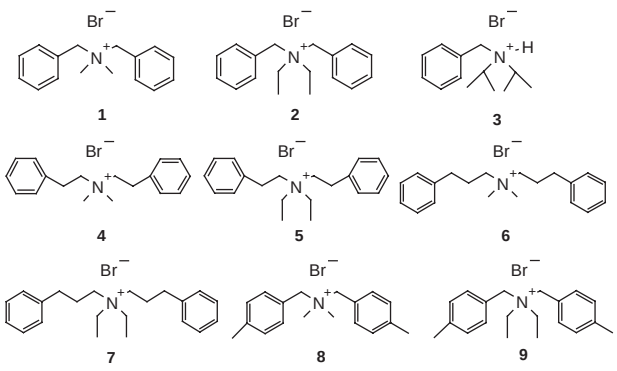

Scheme 1. Molecular structures of compounds **1–9**.

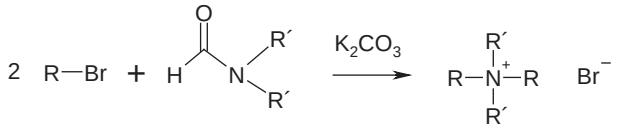

Scheme 2. R = –C_7H_7 (**1–3**), –C_8H_9 (**4–5** and **8–9**), –C_9H_{11} (**6–7**) and R' = –CH_3 (**1,4,6,8**), –C_2H_5 (**2,5,7,9**), –$CH(CH_3)_2$ (**3**). For compound **3** one of the R = H.

2.2. Method A

A small amount of acetone, diethyl ether or methanol was added to the filtrate to give a white or slightly yellow powder. The powder was washed with diethyl ether or acetone and dried in vacuo overnight.

2.3. Method B

The residue was dissolved to water/diethyl ether solution. The water layer was separated and evaporated giving the product as a pure gel. The gel was dried in vacuo.

2.4. Synthesis of dibenzyldimethylammonium bromide (*1*)

Method A. Reagents: benzyl bromide (6.21 mL, 52.25 mmol), potassium carbonate (7.22 g, 52.25 mmol) and dimethylformamide (30 mL). Reaction temperature 80 °C and reaction time 48 h. Yield (white powder) 4.12 g (52%). ^{1}H-NMR (DMSO, 500 MHz, ppm): 2.89 (6H, s, N–C**H**$_3$), 4.70 (4H, s, Ph–C**H**$_2$), 7.50–7.57 (6H, m, Ar–**H**), 7.61–7.63 (4H, m, Ar–**H**). ^{13}C-NMR (DMSO, 126 MHz, ppm): 48.01 (2C, N–**C**H$_3$), 66.86 (2C, Ph–**C**H$_2$), 127.97 (2C, Ar–**C**(1)), 128.84 (4C, Ar–**C**), 130.21 (2C, Ar–**C**(4)), 133.08 (4C, Ar–**C**). Electrospray ionization (ESI)-time of flight (TOF)-MS: m/z calculated for $C_{16}H_{20}NBr$ $[M–Br]^+$: 226.2; found: 226.2 $[M–Br]^+$. Elemental analysis: Calculated for $C_{16}H_{20}NBr$: C, 62.75; H, 6.58; N, 4.57. Found: C, 61.65; H, 6.55; N, 4.39.

2.5. Synthesis of dibenzyldiethylammonium bromide (*2*)

Method A. Reagents: benzyl bromide (5.68 mL, 47.86 mmol), potassium carbonate (9.92 g, 71.79 mmol) and diethylformamide (60 mL). Reaction temperature 50 °C and reaction time 64 h. Yield (white powder) 3.52 g (44%). ^{1}H-NMR (DMSO, 500 MHz, ppm): 1.35 (6H, t (J = 7.16 Hz), N–CH$_2$C**H**$_3$), 3.24 (4H, q (J = 7.16 Hz), N–C**H**$_2$CH$_3$), 4.59 (4H, s, Ph–C**H**$_2$), 7.49–7.56 (6H, m, Ar–**H**), 7.61–7.62 (4H, m, Ar–**H**). ^{13}C NMR (DMSO, 126 MHz, ppm): 8.39 (2C, N–CH$_2$**C**H$_3$), 52.54 (2C, N–**C**H$_2$CH$_3$), 61.73 (2C, Ph–**C**H$_2$), 127.95 (2C, Ar–**C**(1)), 128.94 (4C, Ar–**C**), 130.16 (2C, Ar–**C**(4)), 132.85 (4C, Ar–**C**). ESI-TOF-MS:

m/*z* calculated for $C_{18}H_{24}NBr$ $[M–Br]^+$: 254.2; found: 254.2 $[M–Br]^+$. Elemental analysis: Calculated for $C_{18}H_{24}NBr$: C, 64.67; H, 7.24; N, 4.19. Found: C, 64.34; H, 7.28; N, 4.09.

2.6. Synthesis of benzyldiisopropylammonium bromide (*3*)

Method A. Reagents: benzyl bromide (5.25 mL, 44.16 mmol), potassium carbonate (6.10 g, 44.16 mmol) and diisopropylformamide (22 mL). Reaction temperature 80 °C and reaction time 45 h. Yield (slightly yellow powder) 0.15 g (2%). ^{1}H-NMR (DMSO, 500 MHz, ppm): 1.32 (6H, d (J = 6.61 Hz), N–CH–(C**H**$_3$)$_2$), 1.37 (6H, d (J = 6.61 Hz), N–CH–(C**H**$_3$)$_2$), 3.67–3.70 (2H, m, N–C**H**–(CH$_3$)$_2$), 4.39 (2H, d (J = 5.19 Hz), Ph–C**H**$_2$), 7.44–7.49 (3H, m, Ar–**H**), 7.56–7.58 (2H, m, Ar–**H**), 8.47 (1H, s, N–**H**). ^{13}C NMR (DMSO, 126 MHz, ppm): 17.39 (2C, N–CH–(**C**H$_3$)$_2$), 18.24 (2C, N–CH–(**C**H$_3$)$_2$), 49.64 (1C, Ph–**C**H$_2$), 54.31 (2C, N–**C**H–(CH$_3$)$_2$), 128.68 (2C, Ar–**C**), 129.01 (1C, Ar–**C**(4)), 130.55 (2C, Ar–**C**), 131.66 (1C, Ar–**C**(1)). ESI-TOF-MS: *m*/*z* calculated for $C_{13}H_{22}NBr$ $[M–Br]^+$: 192.2; found: 192.2 $[M–Br]^+$. Elemental analysis: Calculated for $C_{13}H_{22}NBr$: C, 57.36; H, 8.15; N, 5.15. Found: C, 56.75; H, 8.14; N, 5.00.

2.7. Synthesis of dimethyldi-(2-phenylethyl)ammonium bromide (*4*)

Method A. Reagents: 1-bromo-2-phenylethane (8.17 mL, 59.83 mmol), potassium carbonate (8.27 g, 59.83 mmol) and dimethylformamide (25 mL). Reaction temperature 80 °C and reaction time 51 h. Yield (slightly yellow powder) 1.08 g (11%). ^{1}H-NMR (DMSO, 500 MHz, ppm): 3.07–3.10 (4H, m, N–CH$_2$C**H**$_2$–Ph), 3.22 (6H, s, N–C**H**$_3$), 3.59–3.62 (4H, m, N–C**H**$_2$CH$_2$–Ph), 7.26–7.30 (2H, m, Ar–**H**(4)), 7.35–7.38 (8H, m, Ar–**H**). ^{13}C NMR (DMSO, 126 MHz, ppm): 28.13 (2C, N–CH$_2$**C**H$_2$–Ph), 50.03 (2C, N–**C**H$_3$), 63.81 (2C, N–**C**H$_2$CH$_2$–Ph), 126.87 (2C, Ar–**C**(4)), 128.57 (4C, Ar–**C**), 129.00 (4C, Ar–**C**), 136.26 (2C, Ar–**C**(1)). ESI-TOF-MS: *m*/*z* calculated for $C_{18}H_{24}NBr$ $[M–Br]^+$: 254.2; found: 254.2 $[M–Br]^+$. Elemental analysis: Calculated for $C_{18}H_{24}NBr$: C, 64.67; H, 7.24; N, 4.19. Found: C, 63.70; H, 7.15; N, 3.90.

2.8. Synthesis of diethyldi-(2-phenylethyl)ammonium bromide (*5*)

Method A. Reagents: 1-bromo-2-phenylethane (7.54 mL, 55.19 mmol), potassium carbonate (7.63 g, 55.19 mmol) and diethylformamide (30.7 mL). Reaction temperature 80 °C and reaction time 68 h. Yield (slightly yellow powder) 0.44 g (4%). ^{1}H-NMR (DMSO, 500 MHz, ppm): 1.29 (6H, t (J = 7.12 Hz), N–CH$_2$C**H**$_3$), 3.01–3.04 (4H, m, Ph–C**H**$_2$CH$_2$–N), 3.49 (4H, t (J = 7.26 Hz), Ph–CH$_2$C**H**$_2$–N), 3.51 (4H, q (J = 7.12 Hz), N–C**H**$_2$CH$_3$), 7.28–7.31 (2H, m, Ar–**H**), 7.35–7.39 (8H, m, Ar–**H**). ^{13}C NMR (DMSO, 126 MHz, ppm): 7.40 (2C, N–CH$_2$**C**H$_3$), 27.48 (2C, Ph–**C**H$_2$CH$_2$–N), 52.78 (2C, N–**C**H$_2$), 57.35 (2C, N–**C**H$_2$), 126.96 (2C, Ar–**C**), 128.63 (4C, Ar–**C**), 129.01 (4C, Ar–**C**), 136.25 (2C, Ar–**C**). ESI-TOF-MS: *m*/*z* calculated for $C_{20}H_{28}NBr$ $[M–Br]^+$: 282.2; found: 282.2 $[M–Br]^+$. Elemental analysis: Calculated for $C_{20}H_{28}NBr$: C, 66.29; H, 7.79; N, 3.87. Found: C, 64.96; H, 7.72; N, 3.69.

2.9. Synthesis of dimethyldi-(3-phenylpropyl)ammonium bromide (*6*)

Method B. Reagents: 3-phenylpropylbromide (8.39 mL, 55.19 mmol), potassium carbonate (7.63 g, 55.19 mmol) and dimethylformamide (30 mL). Reaction temperature 80 °C and reaction time 72 h. Yield 3.12 g (31%). ^{1}H-NMR (DMSO, 500 MHz, ppm): 1.96 (4H, m, N–CH$_2$C**H**$_2$CH$_2$-Ph), 2.60 (4H, t (J = 7.78Hz), N–CH$_2$CH$_2$C**H**$_2$–Ph), 3.06 (6H, *s*, N–C**H**$_3$), 3.35 (4H, m, N–C**H**$_2$CH$_2$CH$_2$–Ph), 7.21 (2H, m, Ar–**H**(4)), 7.26 (4H, m, Ar–**H**(2,6)), 7.31 (4H, m, Ar–**H**(3,5)). ^{13}C NMR (DMSO, 126 MHz, ppm): 23.53 (2C, N–CH$_2$**C**H$_2$CH$_2$–Ph), 31.52 (2C, N–CH$_2$CH$_2$**C**H$_2$–Ph), 50.16 (2C, N–**C**H$_3$), 62.41 (2C, N–**C**H$_2$CH$_2$CH$_2$–Ph), 126.09 (2C, Ar–**C**(4)), 128.23 (4C, Ar–**C**), 128.31 (4C, Ar–**C**), 140.26 (Ar–**C**(1)). ESI-TOF-MS: *m*/*z* calculated for $C_{20}H_{28}NBr$ $[M–Br]^+$: 282.2; found: 282.2 $[M–Br]^+$. Elemental analysis: Calculated for $C_{20}H_{28}NBr$: C, 66.29; H, 7.79; N, 3.87. Found: C, 64.97; H, 7.95; N, 4.01.

2.10. Synthesis of diethyldi-(3-phenylpropyl)ammonium bromide (*7*)

Method B. Reagents: 3-phenylpropylbromide (7.79 mL, 51.23 mmol), potassium carbonate (7.08 g, 51.23 mmol) and diethylformamide (30 mL). Reaction temperature 80 °C and reaction time 68 h. Yield 1.30 g (13%). ^{1}H-NMR (DMSO, 500 MHz, ppm): 1.09 (6H, t (J = 7.12 Hz), N–CH$_2$C**H**$_3$), 1.86 (4H, m, N–CH$_2$C**H**$_2$CH$_2$–Ph), 2.61 (4H, t (J = 7.56 Hz), N–CH$_2$CH$_2$C**H**$_2$–Ph), 3.15 (4H, m, N–C**H**$_2$CH$_2$CH$_2$–Ph), 3.25 (4H, q (J = 7.12 Hz), N–C**H**$_2$CH$_3$), 7.21 (2H, m, Ar–**H**(4)), 7.26 (4H, m, Ar–**H**(2,6)), 7.31 (4H, m, Ar–**H**(3,5)). ^{13}C NMR (DMSO, 126 MHz, ppm): 7.04 (2C, N–CH$_2$**C**H$_3$), 22.74 (2C, N–CH$_2$**C**H$_2$CH$_2$–Ph), 31.39 (2C, N–CH$_2$CH$_2$**C**H$_2$–Ph), 52.55 (2C, N–**C**H$_2$CH$_3$), 55.97 (2C, N–**C**H$_2$CH$_2$CH$_2$–Ph), 126.18 (2C, Ar–**C**(4)), 128.31 (4C, Ar–**C**), 128.34 (4C, Ar–**C**), 140.23 (2C, Ar–**C**(1)). ESI-TOF-MS: *m*/*z* calculated for $C_{22}H_{32}NBr$ $[M–Br]^+$: 310.3; found: 310.2 $[M–Br]^+$. Elemental analysis: Calculated for $C_{22}H_{32}NBr$: C, 67.68; H, 8.26; N, 3.59. Found: C, 67.95; H, 8.38; N, 3.69.

2.11. Synthesis of dimethyldi-(4-methylbenzyl)ammonium bromide (8)

Method A. Reagents: 4-methyl benzyl bromide (9.00 g, 48.63 mmol), potassium carbonate (6.20 g, 44.87 mmol) and dimethylformamide (30 mL). Reaction temperature 80 °C and reaction time 50 h. Yield (slightly yellow powder) 3.25 g (40%). ^{1}H-NMR (DMSO, 500 MHz, ppm): 2.36 (6H, s, Ph–C**H**$_3$), 2.85 (6H, s, N–C**H**$_3$), 4.62 (4H, s, Ph–C**H**$_2$), 7.32 (4H, d (J = 7.93 Hz), Ar–**H**), 7.49 (4H, d (J = 8.01 Hz), Ar–**H**). ^{13}C NMR (DMSO, 126 MHz, ppm): 20.78 (2C, Ph–**C**H$_3$), 47.79 (2C, N–**C**H$_3$), 66.55 (2C, Ph–**C**H$_2$), 124.98 (2C, Ar–**C**), 129.39 (4C, Ar–**C**), 132.94 (4C, Ar–**C**), 139.84 (2C, Ar–**C**). ESI-TOF-MS: m/z calculated for $C_{18}H_{24}NBr$ [M–Br]$^+$: 254.2; found: 254.2 [M–Br]$^+$. Elemental analysis: Calculated for $C_{18}H_{24}NBr$: C, 64.67; H, 7.24; N, 4.19. Found: C, 63.37; H, 7.04; N, 3.68.

2.12. Synthesis of diethyldi-(4-methylbenzyl)ammonium bromide (9)

Method B. Reagents: 4-methyl benzyl bromide (8.17 g, 44.16 mmol), potassium carbonate (6.10 g, 44.16 mmol) and diethylformamide (25 mL). Reaction temperature 80 °C and reaction time 45 h. Yield 2.21 g (28%). ^{1}H-NMR (DMSO, 500 MHz, ppm): 1.34 (6H, t (J = 7.16 Hz), N–CH$_2$C**H**$_3$), 2.35 (6H, s, Ph–C**H**$_3$), 3.20 (4H, q (J = 7.16 Hz), N–C**H**$_2$CH$_3$), 4.54 (4H, s, N–C**H**$_2$–Ph), 7.31 (4H, d (J = 7.78 Hz), Ar–**H**), 7.49 (4H, d (J = 8.11 Hz), Ar–**H**). ^{13}C NMR (DMSO, 126 MHz, ppm): 8.40 (2C, N–CH$_2$**C**H$_3$), 20.73 (2C, Ph–**C**H$_3$), 52.25 (2C, N–**C**H$_2$CH$_3$), 61.33 (2C, N–**C**H$_2$-Ph), 124.94 (2C, Ar–**C**), 129.48 (4C, Ar–**C**), 132.71 (4C, Ar–**C**), 139.77 (2C, Ar–**C**). ESI-TOF-MS: m/z calculated for $C_{20}H_{28}NBr$ [M–Br]$^+$: 282.2; found: 282.2 [M–Br]$^+$. Elemental analysis: Calculated for $C_{20}H_{28}NBr$: C, 66.29; H, 7.79; N, 3.87. Found: C, 64.89; H, 7.89; N, 4.12.

2.13. Characterization

The formation of produced quaternary ammonium bromides was confirmed by ^{1}H and ^{13}C NMR and also by ESI TOF MS. ^{1}H-NMR spectra and ^{13}C-NMR spectra were measured in DMSO at 30 °C by using a Bruker Avance DRX 500 NMR spectrometer operating at 500 MHz for ^{1}H and 126 MHz for ^{13}C. Electrospray mass spectrometric measurements were made by using the Micromass LCT TOF mass spectrometer with ESI. All the compounds were measured by using positive mode with sample concentrations in methanol solution, as follows: (25 mg/L) except for compound **3** (500 mg/L). The elemental analyses were carried out with Vario EL III CHN elemental analyzer by using dried sample weights of 3–5 mg.

2.14. Structure analysis

The X-ray structures for compounds **1**–**5** and **8** were determined by X-ray single crystal diffraction and for compound **1** also by X-ray powder diffraction [54]. The powder structure determination details for compound **1** are presented elsewhere [41]. Colorless single crystals of compounds **1**–**5** and **8** were produced by recrystallization from MeOH/EtAc solution. Crystallographic data for those compounds were obtained with a Nonius KappaCCD diffractometer at −100 °C using graphite monochromaticed Mo$K\alpha$ ($\lambda = 0.71069$ Å) radiation. The data were processed with EvalCCD [55] software package and the absorption correction was made by SADABS (included in EvalCCD software package). All the structures were solved by using direct methods (SIR2002 [56] or SHELXS-97 [57]) and refined on F^2 by full-matrix least-squares techniques (SHELXL-97 [58]) by using anisotropic temperature factors. All the hydrogen atoms were calculated to their positions as riding atoms by using isotropic temperature factors.

In case of crystalline compounds, the powder diffraction data were measured to confirm the expected structural similarity of the single crystals and the microcrystalline bulk materials. High-resolution X-ray powder diffraction data were obtained at 22 °C by Huber G670 imaging-plate Guinier camera. The sealed-tube X-ray generator system was operated at 45 kV and 25 mA and pure line-focused Cu$K\alpha_1$ radiation ($\lambda = 1.5406$ Å) was produced by primary beam curved germanium monochromator ($d = 3.266$ Å). The measurement was carried out in Guinier-type transmission geometry with the angle of incidence 45° to the sample normal. The handground samples were prepared on the vaseline-coated Mylar foil of 3.5 μm thickness. The diffracted X-ray photons with the angular range of 4–100° (2θ) were captured to the curved imaging plate detector. The diffraction data were acquired from the detector by step scanning laser with step size of 0.005° (2θ). The measurement time for the samples varied between 20 and 60 min.

2.15. Thermal properties

Melting points for the compounds **1**–**5** and **8** were determined both on Mettler Toledo FP62 melting point instrument (not corrected) and on PerkinElmer PYRIS Diamond DSC. The DSC measurements were carried out using 50 μL aluminum sample pans with pinholes. The temperature calibration was made using three standard materials (*n*-decane, In, Zn) and the energy calibration by indium standard. The samples were heated with a rate of 10 °C/min from −40 °C near the

predetermined (DSC, TG/DTA) decomposition temperature of each compound. In some cases more detailed DSC scans were carried out by using two heating–cooling cycles and/or slower cooling rate of 2–5 °C/min. The sample weights used in the measurements were about 4 mg.

The thermal decomposition paths for compounds **1–9** were obtained with PerkinElmer Diamond TG/DTA. Measurements were carried out using platinum pans under synthetic air atmosphere (flow rate of 110 mL/min) at temperature range 20–400 °C (heating rate of 10 °C/min). The temperature calibration of TG/DTA equipment was carried out using melting points of five reference materials (In, Sn, Zn, Al, Au). The weight balance was calibrated by measuring the standard weight as a function of temperature. The sample weights used in the measurements were about 6 mg.

3. Results and discussion

3.1. Characterization

The formation of quaternary ammonium bromides was easily confirmed with ^{1}H-NMR and ^{13}C-NMR. The characterizations carried out with mass spectrometry showed unequivocally the formation of the desired quaternary compound. In all cases except for compound **3**, the most intense peak corresponded to the isolated cation. Furthermore, the next most intense peak originated from the $\{(\text{cation})_2\text{Br}\}^+$, whose intensity was about 20% of the isolated cation peak. Somewhat deviating behavior was obtained on compound **3**, as the $\{(\text{cation–H})_2\text{Br}\}^+$ ($m/z = 463$) peak was most intense, following the next most intense peak of isolated cation (intensity of 80% that of the most intense peak). It is assumed that the formation of cation dimer is favored due to the cleavage of N…H hydrogen (HBr formation). The elemental analyses were satisfactory in all cases, although slightly lower values were obtained systematically. However, traces of water were expected to reside in the samples despite of the drying in vacuo, as the compounds proved to be somewhat hygroscopic thus some water could be taken up by the samples during sample preparation. In fact, the calculated values corresponded well to the found values if $\frac{1}{4}$ or less H_2O was added to molecular weights.

3.2. Structure analysis

The colorless single crystals of compounds **1–5** and **8** were grown by slow evaporation from MeOH/EtAc solution. The crystallographic data are shown in Table 1. The selected bond lengths and angles are gathered in Table 2.

Table 1
Crystallographic data for compounds **1–5** and **8**

Compound	**1**	**2**	**3**	**4**	**5**	**8**
Formula	$C_{16}H_{20}NBr$	$C_{18}H_{24}NBr$	$C_{13}H_{22}NBr$	$C_{18}H_{24}NBr$	$C_{20}H_{28}NBr$	$C_{18}H_{24}NBr$
M_r (g/mol)	306.24	334.29	272.23	334.29	362.34	334.29
Crystal system	Monoclinic	Orthorhombic	Monoclinic	Triclinic	Orthorhombic	Monoclinic
Space group	$P2_1/c$	$Pbca$	$P2_1/c$	$P\bar{1}$	$P2_12_12_1$	$C2/c$
a (Å)	13.023(1)	14.532(5)	13.640(1)	5.8924(3)	7.300(5)	6.535(5)
b (Å)	10.309(1)	12.847(5)	8.439(1)	7.6270(4)	10.176(5)	15.452(5)
c (Å)	10.826(3)	35.628(6)	12.509(1)	17.753(1)	24.573(5)	16.490(5)
α (°)	90	90	90	85.72(1)	90	90
β (°)	91.84(1)	90	110.40(4)	87.52(1)	90	97.21(1)
γ (°)	90	90	90	89.59(1)	90	90
V (Å^3)	1452.7(4)	6652(3)	1349.5(2)	794.9(1)	1825(2)	1652(2)
Z	4	16	4	2	4	4
ρ_{calcd} (g/cm^3)	1.400	1.335	1.340	1.397	1.318	1.344
μ (mm^{-1})	2.813	2.463	3.018	2.577	2.250	2.480
F (000)	632	2784	568	348	760	696
Crystal size (mm)	0.4 × 0.2 × 0.2	0.3 × 0.1 × 0.1	0.15 × 0.10 × 0.10	0.50 × 0.40 × 0.20	0.20 × 0.15 × 0.10	0.40 × 0.25 × 0.15
θ range (deg)	3.12–25.00	3.03–25.01	3.07–25.00	3.40–25.00	3.19–25.00	3.41–24.97
Reflections collected	11421	42501	10378	11283	10023	5645
Independent reflections	2557	5848	2366	2759	3171	1449
Data/restraints/parameters	2557/0/164	5848/0/361	2366/0/140	2759/0/181	3171/0/200	1449/0/93
GooF	1.010	1.012	0.993	1.039	0.940	1.035
R (int)	0.0637	0.1783	0.0952	0.0400	0.0915	0.0730
Final R indices [$I > 2\sigma(I)$]	$R_1 = 0.0345$	$R_1 = 0.0559$	$R_1 = 0.0414$	$R_1 = 0.0287$	$R_1 = 0.0461$	$R_1 = 0.0445$
	$wR_2 = 0.0454$	$wR_2 = 0.0667$	$wR_2 = 0.0531$	$wR_2 = 0.0513$	$wR_2 = 0.0570$	$wR_2 = 0.0844$
R indices (all data)	$R_1 = 0.0773$	$R_1 = 0.1501$	$R_1 = 0.1094$	$R_1 = 0.0448$	$R_1 = 0.1288$	$R_1 = 0.0924$
	$wR_2 = 0.0510$	$wR_2 = 0.0816$	$wR_2 = 0.0624$	$wR_2 = 0.0543$	$wR_2 = 0.0700$	$wR_2 = 0.0957$
Largest diff. peak/hole (e/Å^3)	0.297/−0.306	0.543/−0.427	0.356/−0.469	0.275/−0.374	0.349/−0.323	0.524/−0.455

Table 2
Selected bond lengths (Å) and bond angles (deg) for compound **1**–**5** and **8**

Compound	**1**	**2**	**3**	**4**	**5**	**8**
N(1)–C(11)	1.532(3)	1.524(5)	1.516(4)	1.510(3)	1.523(5)	1.541(4)
N(1)–C(21)	1.528(3)	1.531(5)	1.528(4)	1.516(3)	1.510(5)	1.486(4)
N(1)–C(31)	1.490(3)	1.538(6)	1.543(4)	1.500(3)	1.525(5)	1.541(4)
N(1)–C(41)	1.495(3)	1.506(5)	—	1.504(3)	1.521(5)	1.486(4)
C(11)–N(1)–C(21)	106.7(2)	107.6(3)	111.5(3)	113.5(2)	111.4(3)	109.7(2)
C(11)–N(1)–C(31)	110.3(2)	111.8(4)	111.3(3)	107.1(2)	110.7(3)	105.9(4)
C(11)–N(1)–C(41)	109.6(2)	108.9(4)	—	111.0(2)	106.1(3)	110.9(2)
C(21)–N(1)–C(31)	109.5(2)	104.3(3)	113.9(3)	110.2(2)	106.4(3)	110.9(2)
C(21)–N(1)–C(41)	110.5(2)	111.3(3)	—	106.9(2)	111.5(4)	109.7(4)
C(31)–N(1)–C(41)	110.1(2)	112.9(4)	—	108.0(2)	110.8(3)	109.7(2)

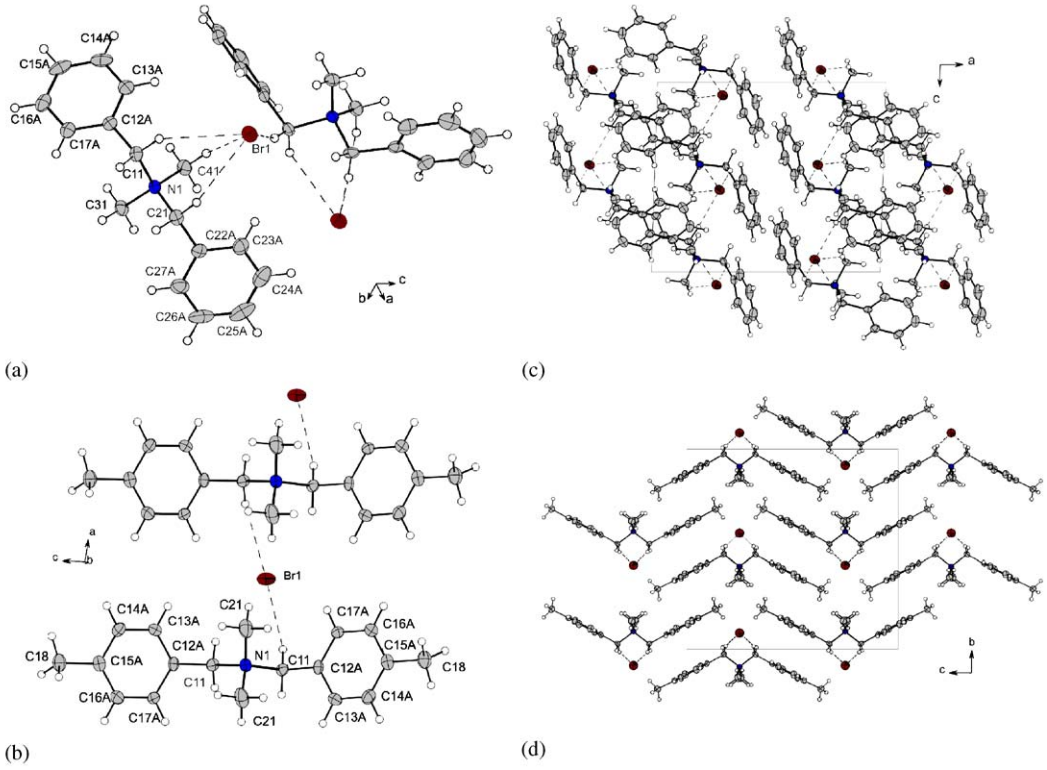

Fig. 1. The ion-pair ordering and hydrogen bonding (<3.05 Å) of compounds **1** (a) and **8** (b). The packing mode of both compounds (c) and (d) show face to face $\pi-\pi$ interaction between phenyl rings. For **1** the shortest cation/anion distances are Br1…C41* 3.864(3), Br1…C21* 3.804(3) and Br1…C11* 3.709(17) and to all the adjacent nitrogen atoms about 4.11 Å; and for **8** Br1…C11* 3.775(7), Br1…C11** 3.957(6) and to the adjacent nitrogen atoms about 4.17 Å, respectively. Symbols **1)** * = x, 0.5−y, −0.5+z, and **8)** * = −1+x, y, z; ** = 1−x, y, 1.5−z, indicate symmetry operations to generate nearby atoms.

Compounds **1** and **3** crystallized in monoclinic space group $P2_1/c$, compound **8** in monoclinic space group $C2/c$ and compound **4** in triclinic space group P-1. Compounds **2** and **5** crystallized in orthorhombic space groups *Pbca* and $P2_12_12_1$ (Flack parameter = 0.01(1)), respectively. Despite several attempts, we have not been able to crystallize the compounds **6**, **7** and **9** (viscous oil **6**, waxy **7** and **9**), although based on the NMR, MS and TG/DTA studies compounds were free of solvents and other impurities. For the solved crystal structures, the ion-pair ordering and the crystal packing are presented in Figs. 1–3 [59].

In case of compounds **1** and **8** the cation appears in W-conformation so that the methyl groups are between the phenyl groups (Fig. 1). The cation/anion pairs are interconnected by weak Br^-…H bonding, bond distances varying 2.97–3.05 Å for **1** and 2.84 Å for **8**. Furthermore, the ion pairs are packed via intermolecular

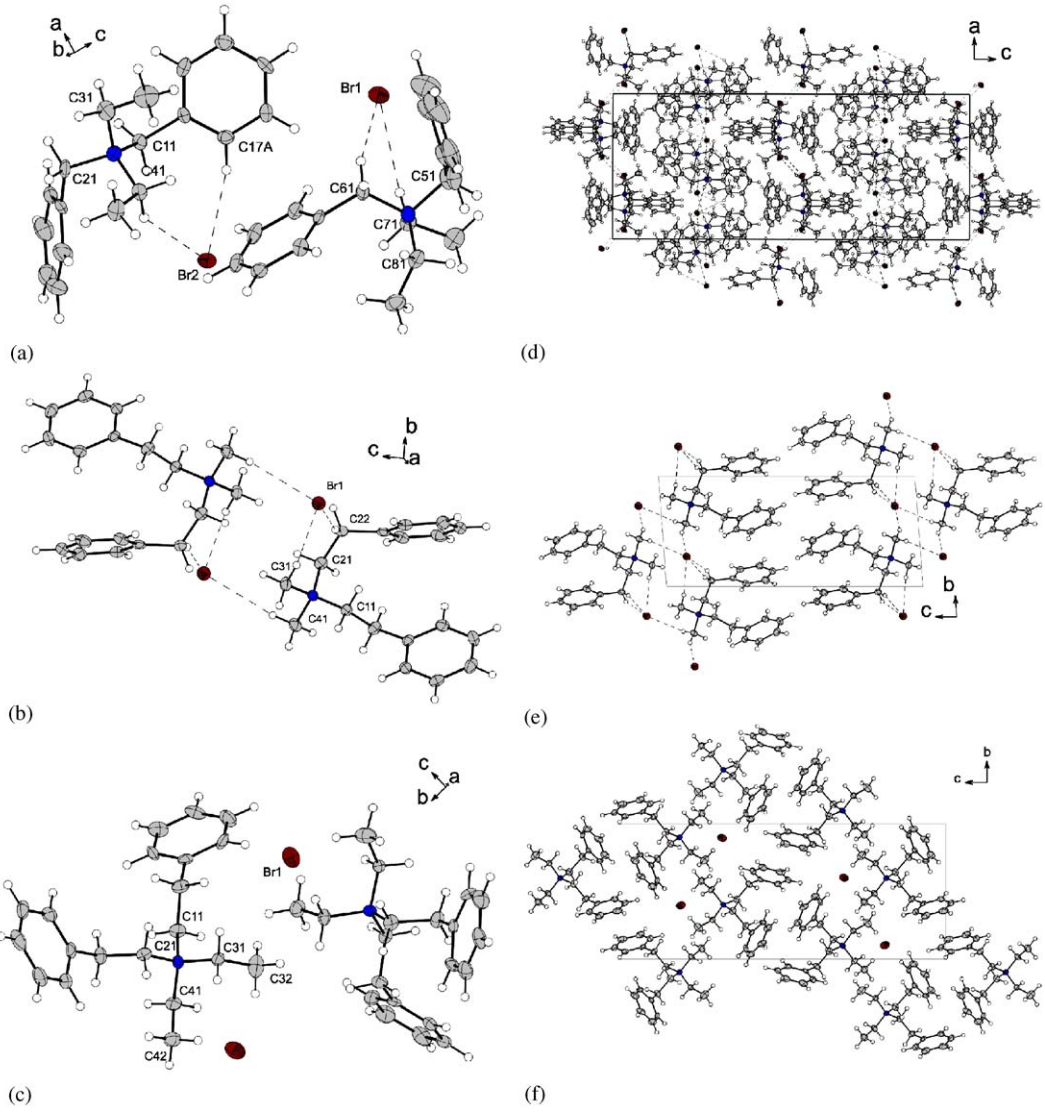

Fig. 2. The ion-pair ordering and hydrogen bonding (<3.05 Å) of the compounds **2** (a), **4** (b) and **5** (c). The packing modes of compounds **2** (d), **4** (e), and **5** (f) show edge to face $\pi-\pi$ interaction between the phenyl rings. For **2**, the shortest cation/anion distances are Br2…C11* 3.631(5), Br2…C17A 3.720(4), and Br1…C81** 3.644(5) and to the adjacent nitrogen atoms about 4.15 Å; for **4**, Br1…C41* 3.691(8), Br1…C22** 3.703(8), and Br1…C31** 3.766(8) and to the nitrogen atoms about 4.30 Å; for **5**, Br1…C42* 3.662(5), Br1…C32** 3.846(5), and Br1…C32 3.873(5) and to the nitrogen atoms about 4.72 Å, respectively. Symbols **2)** * $=-0.5+x$, y, $0.5-z$; ** $=1.5-x$, $-0.5+y$, z, **4)** * $=-x$, $2-y$, $-z$; ** $=1+x$, y, z, and **5)** * $=x$, $-1+y$, z; ** $=2-x$, $-0.5+y$, $1.5-z$, indicate symmetry operations required to generate nearby atoms.

face to face $\pi-\pi$ interactions between the phenyl groups [60,61]. In compound **8** the cations are tightly interlocked, so that both phenyl groups of the cation participate in $\pi-\pi$ interactions, therefore further stabilizing the crystal packing.

The asymmetric unit of **2** consists of two cation/anion pairs (Fig. 2a), in which the ion pairs are interconnected similarly as presented for compounds **1** and **8**, bond distances varying from 2.69 to 2.95 Å. Furthermore, the molecular packing is stabilized by both intramolecular CH…π interaction and intermolecular edge to face $\pi-\pi$ interaction. The ion-pair interactions and hydrogen bond distances (2.77–2.94 Å) of compound **4** are analogous to previous compounds. Two phenyl rings of the cation are strongly turned towards each other forming continuous and alternating edge to face $\pi-\pi$ bonding, in which every second connection between phenyl rings is intramolecular and the other intermolecular (Fig. 2e). As the phenyl rings are in close proximity to each other and the fact that rings are located on the center section of the unit cell layer-like structure is formed. The packing of compound **5** is most spacious as no clear hydrogen bonds (<3.05Å) were found and the average $N^+ \ldots Br^-$ distance was about 4.7 Å (about 4.2 Å for the rest of compounds, except for **3**). The phenyl rings showed intermolecular edge to face $\pi-\pi$

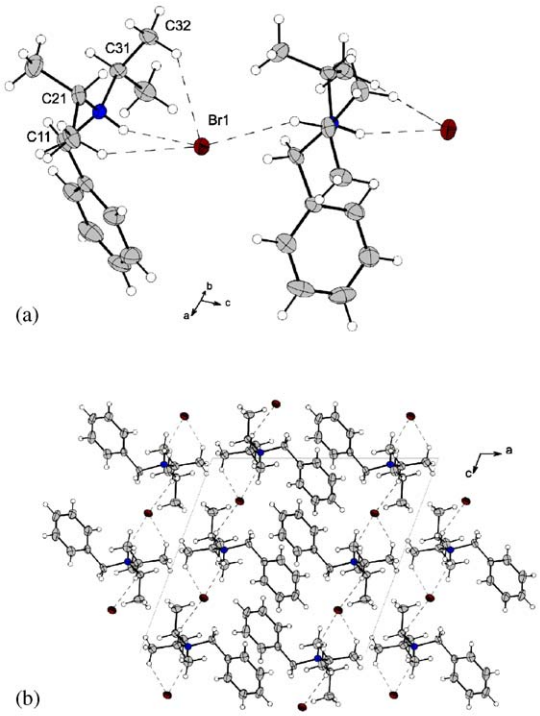

Fig. 3. The ion-pair ordering and hydrogen bonding (<3.05 Å) of compound **3** (a) and the packing mode (b) showing face to face $\pi-\pi$ interaction between the phenyl rings. The shortest cation/anion distances are Br1…C32 3.696(7), Br1…C31 3.709(4), and Br1…C21 3.746(5) and to the adjacent nitrogen atoms about 3.31 Å.

bonding (Fig. 2f). As expected, the melting point of compound **5** was lowest among the crystallized compounds.

In case of compound **3**, as the desired compound (R'_2R_2NBr) was not produced, various analyses were carried out by NMR from the mother liquid, precipitates and from the liquid extracted by evaporator to search out the presence of the expected quaternary ammonium salt. However, no sign was detected, which could confirm the presence of the desired quaternary salt. It is assumed that the reactivity of intermediate cation was lowered (due to steric effects) excessively during the synthesis preventing the reaction between the intermediate cation and the second benzyl group, which then was overtaken by distinctively smaller hydrogen atom. The ion pair of compound **3** is interconnected via hydrogen bond between the bromide and the N^+–H hydrogen (2.50 Å) and with weaker hydrogen bonds (2.89–3.01 Å) between the hydrogen atoms of isopropyl groups and bromide (Fig 3a). The packing of **3** is quite similar to the packing of compounds **1** and **8**. However, the single phenyl ring of each cation is paired with the phenyl ring of the next cation across the unit cell by face to face type $\pi-\pi$ interaction causing the isopropyl groups to face towards bromide anions resembling the layer-like structure of compound **4**.

3.3. Powder diffraction analysis

The powder diffraction data were measured to confirm the expected similarities of the single crystals and the microcrystalline bulk material. The calculated powder data were obtained from the structural parameters of each of the compounds by CRYSTALLOGRAPHICA [62] software package. The comparison of the experimental and calculated data is presented in Fig. 4. Based on the powder diffraction analyses, the structural ordering of microcrystalline bulk materials and the single crystals were congruent in all cases. Furthermore, the crystallinity of compounds **1–5** and **8** was relatively high as quite narrow half-widths with high overall intensity gains were observed on experimental powder data.

3.4. Thermal analysis

The results of DSC measurements for compounds **1–9** are summarized in Table 3. The transition temperatures were taken from the peak onsets. Analogous melting points were observed also by Melting point apparatus and on TG/DTA. The TG/DTA curves for **1–9** are presented in Fig. 5.

Based on the TG/DTA and DSC studies, the decomposition of the compounds **1–2** and **8** started during or even slightly before the melting. Therefore, the observed transitions at 175 (**1**), 174 (**2**) and 202 °C (**8**) are somewhat fictitious melting points. Compound **9** has narrow liquid range as melting point (T_m) was observed at 131.3 °C, just before the decomposition started. Compounds **3–5** and **7** melted at 158.6, 158.1, 122.2 and 109.1 °C, respectively, and isotropic liquid range of 30–70 °C was observed for these compounds prior to the decomposition. The thermal studies for **6** suggested that compound stayed in liquid state from −40 to about 180 °C, from which the decomposition started. In general, all the compounds decomposed without identifiable cleavages and the starting of the decomposition varied between 165 and 190 °C, except for **9** that started to decompose at 135 °C.

For compound **4**, three transition signals were observed between 146 and 158 °C both in DSC and TG/DTA measurements. It is assumed that the room temperature phase melted at 146 °C and almost simultaneously recrystallized (partly overlapping peak with onset at 150 °C) to the second polymorph, which then melted at 158 °C. More detailed DSC measurements with two heating–cooling cycles showed that on the first cooling scan only a weak glass transition was observed, indicating the amorphous solidification of the compound. On subsequent heating, both glass transition (24.0 °C) and crystallization (73.2 °C) was observed.

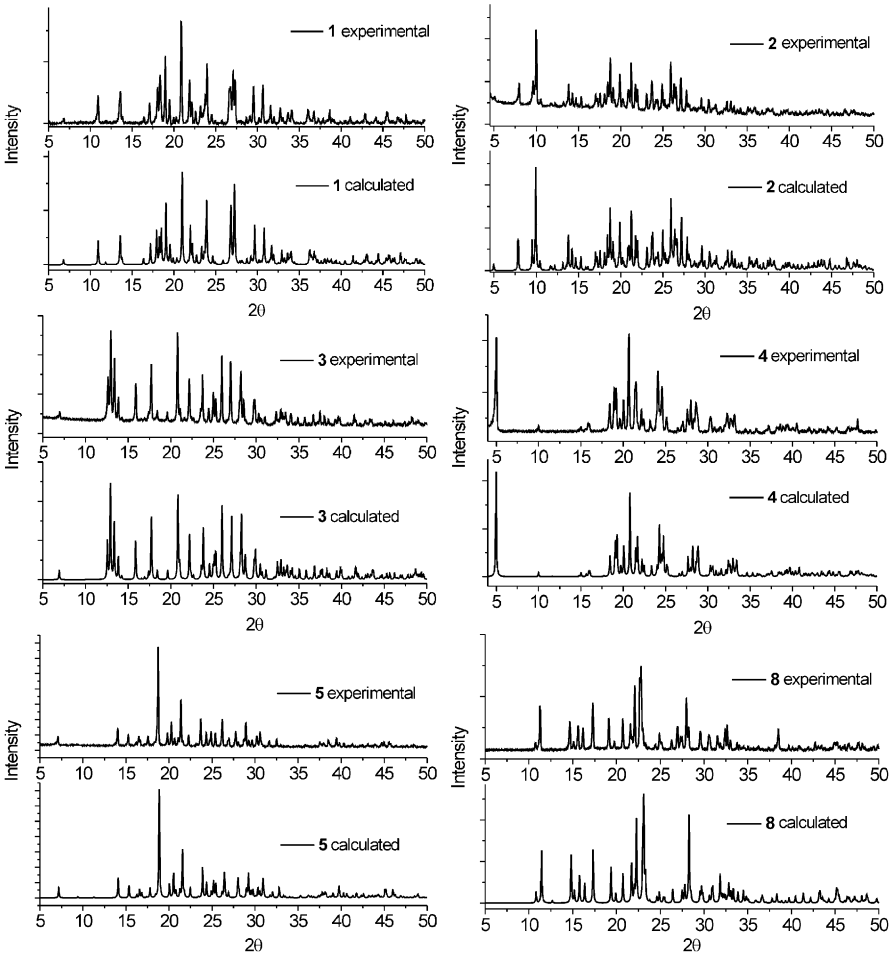

Fig. 4. Experimental powder data compared with calculated data which were obtained from the single crystal structure parameters. Pseudo-voigt function (peak profile parameters $U = 0$, $V = 0.01$ and $W = 0.01$) and Cu$K\alpha_1$ wavelength was used on calculations.

Table 3
Melting points (onset), decomposition ranges (starting value taken from initial mass loss of the decomposition; T_i) and enthalpy changes for compounds **1**–**9**

Compound	T_m (onset) (°C)	Enthalpy change (kJ/mol)	Decomposition range (°C)
1	175[a]	23.3	165–245
2	174[a]	30.2	164–232
3	158.6	24.1	189–290
4	145.5[b], 158.1	17.9	192–302
5	122.2	25.7	191–305
6	—	—	180–300
7	109.1	17.4	178–316
8	202[a]	14.1	190–270
9	131.3	9.1	135–300

[a]Not definite T_m as compounds decomposed during melting.
[b]Lower T_m corresponds to the room-temperature phase.

Originally, it was assumed that by changing the methyl groups of the cation, which originated from the amide, to the larger groups and secondly by lengthening the carbon chain between the nitrogen and phenyl ring, the thermal properties of the compounds could be modified. For compounds **1** and **2**, the effect of changing the methyl groups to the ethyl groups was rather weak as the decomposition/melting of these compounds started nearly at the same temperature (175 °C). First, noticeable decrease on T_m was observed with compounds **4** and **5** as latter melted about 35 °C lower than compound **4**. However, clearer decreasing trend of melting points (T_m of **2**>**5**>**7** for diethyl compounds and **1**>**4**>**6** for dimethyl compounds) was observed when the carbon chain between the phenyl ring and the nitrogen was lengthened and by this the lowest T_m was obtained for **7** (109 °C). Furthermore, compound **6** deviated significantly from the rest of the group since it appeared as a viscous liquid despite of the several attempts to solidify/crystallize the compound. If compounds **6** and **7** are considered from the structural point of view, the cation of **7** could be more rigid, as the mobility of the 3-phenylpropyl groups may be limited in larger extent by the ethyl groups than in case of **6** having smaller methyl groups thus with more rigid branches

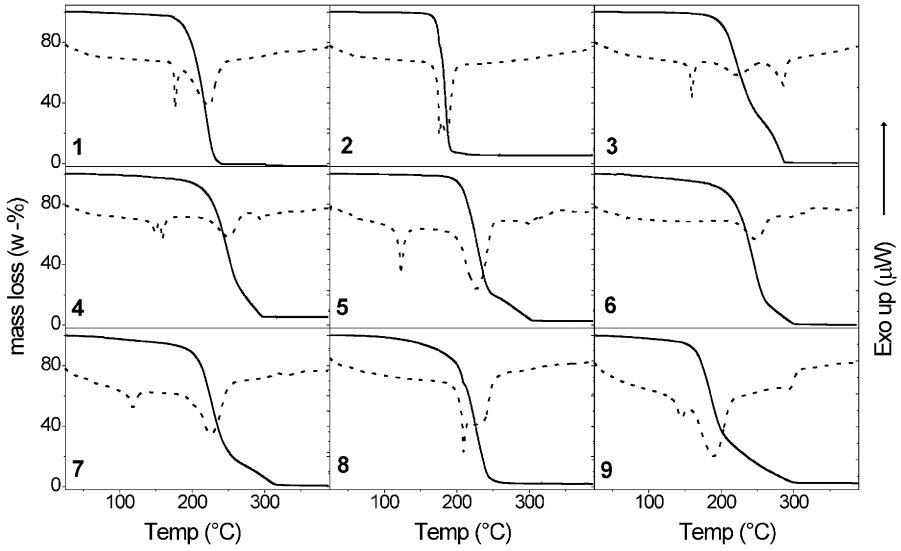

Fig. 5. TG/DTA curves for compounds **1**–**9**. The exothermic events are pointing up in DTA curves. The TG curves are presented by solid lines and DTA curves as dashed lines, respectively.

the long-range ordering of the ion pairs can occur more easily.

4. Conclusions

Eight new aromatic $R_2R'_2N^+Br^-$-type (R = benzyl, 4-methylbenzyl, 2-phenylethyl, 3-phenylpropyl; R' = ethyl, methyl, isopropyl) and one $RR'_2NH^+Br^-$-type (R = benzyl; R' = isopropyl) quaternary ammonium bromides were prepared by using novel synthetic route in which diethylformamide, dimethylformamide or diisopropylformamide were treated with selected aralkyl halide in presence of potassium carbonate. Six of the compounds were crystalline and their single crystal structures were solved and their structural similarities with microcrystalline bulks were confirmed by the powder diffraction studies. The thermal properties of the compounds were changed by increasing the carbon chain length between the phenyl ring and nitrogen and by changing the methyl groups to the ethyl groups. The low melting points of salts **5** and **7** along with broad liquid ranges (about 70 °C) and very broad liquid range up to the decomposition temperature (180 °C) of compound **6** (viscous liquid) enable the potential applicability of these three compounds as ionic liquids, which is to be tested along with anion exchange, in further studies. Compounds **3** and **4** melted roughly at 158 °C having liquid range of about 30 °C above the T_m, but the liquid ranges above 150 °C are in some extent less applicable, for example, as organic solvents. Quite low T_m was observed for salt **9** also, but unfortunately the decomposition of the compound followed readily after melting.

All the compounds were soluble in water but as the hydrocarbon content of the cation increased, the solubility behavior changed due to an increased proportion of the hydrophobic cation compared to the hydrophilic anion. This phenomenon could be exploited in phase-transfer-catalyzed processes, as both types of solubility properties are needed at the boundary layer of the reaction mixture. Finally, the presented quaternary ammonium compounds may be interesting guests for studies of complexation, capsule formation and crystal engineering purposes with resorcinarenes, as the electron-rich resorcinarene cavity is known to complexate both small quaternary alkyl ammonium cations via cation–π interactions, and planar aromatic guests by $\pi-\pi$ interactions [25–28,63].

Acknowledgments

We thank Mr. Reijo Kauppinen and Prof. Erkki Kolehmainen for measuring the NMR spectra and Ms. Elina Hautakangas and Ms. Ritva Watia for measuring the elemental analysis data. K.R. gratefully acknowledges the financial support by the National Technology Agency (TEKES, proj. no. 40004/01) and S.B. correspondingly the Faculty of Mathematics and Science of University of Jyväskylä.

Supporting information available

Crystallographic data for the structures reported in this paper have been deposited with the Cambridge Crystallographic Data Center as supplementary publication no. CCDC_227627–227632. Copies of the data can be obtained free of charge on application to CCDC, 12 Union Road, Cambridge CB2 1EZ, UK

(Fax: +44-1223-336-033; E-mail: deposit@ccdc.cam.ac.uk).

References

[1] N. Muto, K. Fushiya, Patent, Jpn. Kokai Tokkyo Koho, 2002.
[2] F. Menger, J. Keiper, Angew. Chem. Int. Ed. 39 (2000) 1907–1920.
[3] M. In, V. Bec, O. Aguerre-Chariol, R. Zana, Langmuir 16 (2000) 141–148.
[4] T. Ooi, Y. Uematsu, M. Kameda, K. Maruoka, Angew. Chem. Int. Ed. 41 (2002) 1551–1554.
[5] X. Li, S. Goh, Y. Lai, S.-M. Deng, J. Appl. Polym. Sci. 73 (1999) 2771–2777.
[6] S. Jacobson, Patent, US, 1998.
[7] L. Tagle, F. Diaz, C. San Martin, Bol. Soc. Chil. Quim. 38 (1993) 27–30.
[8] W. Lunsmann, V. Villa, Patent, Eur. Pat. Appl., 2001.
[9] J. Shirai, T. Kanno, Y. Tsuchiya, S. Mitsubayashi, R. Seki, J. Vet. Med. Sci. 62 (2000) 85–92.
[10] S. Guzzo, R. Harakava, K. Kida, E. Martins, D. Roveratti, Summa Phytopathol. 25 (1999) 339–345.
[11] M. Hayama, A. Asai, Patent, Jpn. Kokai Tokkyo Koho, 1998.
[12] L. Taylor, M. Sivik, A. Willey, J. Burckett-St. Laurent, F. Hartman, Patent, Eur. Pat. Appl., 1996.
[13] V. Siqueira, Patent, Braz. Pedido PI, 1996.
[14] C. Wright, P. Brougham, Patent, PCT Int. Appl., 1994.
[15] P. Kassentini, Patent, Fr. Demande, 1994.
[16] R. Login, J. Merianos, Patent, US, 1993.
[17] H. Martin, Patent, US, 1994.
[18] H. Kikuyama, H. Izumi, Y. Kikunaga, M. Miyashita, Patent, PCT Int. Appl., 2001.
[19] S. Senoo, K. Noda, Patent, Jpn. Kokai Tokkyo Koho, 1997.
[20] K. Noda, E. Endo, K. Takahashi, Patent, Jpn. Kokai Tokkyo Koho, 1995.
[21] K. Noda, K. Takahashi, K. Tanaka, H. Watanabe, K. Hikuma, Patent, Jpn. Kokai Tokkyo Koho, 1994.
[22] E. Turner, C. Pye, R. Singer, J. Phys. Chem. A 107 (2003) 2277–2288.
[23] P. Wasserscheid, W. Keim, Angew. Chem. Int. Ed. 39 (2000) 3772–3789.
[24] A. Abbott, D. Davies, Patent, PCT Int. Appl., 2000.
[25] H. Mansikkamäki, M. Nissinen, C. Schalley, K. Rissanen, New. J. Chem. 27 (2003) 88–97.
[26] H. Mansikkamäki, M. Nissinen, K. Rissanen, Chem. Commun. 17 (2002) 1902–1903.
[27] K. Murayama, A. Katsuyuki, Chem. Commun. 5 (1998) 607–608.
[28] A. Shivanyuk, J. Rebek, Chem. Commun. 22 (2001) 2374–2375.
[29] T. Stevens, E. Creighton, A. Gordon, M. MacNicol, J. Chem. Soc. (1928) 3193–3197.
[30] T. Stevens, J. Chem. Soc. (1930) 2107–2119.
[31] T. Stevens, W. Snedden, E. Stiller, T. Thomson, J. Chem. Soc. (1930) 2119–2125.
[32] T. Thomson, T. Stevens, J. Chem. Soc. (1932) 55–69.
[33] T. Thomson, T. Stevens, J. Chem. Soc. (1932) 69–73.
[34] J. Dunn, T. Stevens, J. Chem. Soc. (1932) 1926–1931.
[35] T. Thomson, T. Stevens, J. Chem. Soc. (1932) 1932–1940.
[36] K. Agagi, S. Oae, M. Murakami, J. Am. Chem. Soc. 79 (1957) 3118–3120.
[37] K. Laidler, C. Hinshelwood, J. Chem. Soc. (1938) 858–862.
[38] S. Haas, H. Hoffmann, Prog. Polym. Sci. 101 (1996) 131–134.
[39] H. Rutzen, P. Lorenz, H. Tesmann, Eur. Pat. Appl., 1988.
[40] J. Miller, J. Sauer, D. DeLaet, Patent, US, 1997.
[41] J. Ropponen, M. Lahtinen, S. Busi, M. Nissinen, E. Kolehmainen, K. Rissanen, New J. Chem., in press.
[42] S. Nemeth, A. Robinson, N. Campbell, Abstracts of Papers, 226th ACS National Meeting, New York, NY, United States, September 7–11, 2003.
[43] M. Uzagare, M.Y. Sanghvi, M. Salunkhe, Green Chem. 5 (2003) 370–372.
[44] E. Hassoun, M. Abraham, V. Kini, M. Al-Ghafri, A. Abushaban, Res. Commun. Pharmacol. Toxicol. 7 (2002) 23–31.
[45] A. Riisager, R. Fehrmann, R. van Hal, P. Wasserscheid, Abstracts of Papers, 226th ACS National Meeting, New York, NY, United States, September 7–11, 2003, IEC-042.
[46] J. Revell, A. Ganesan, Org. Lett. 4 (2002) 3071–3073.
[47] R. Brown, P. Dyson, D. Ellis, T. Welton, Chem. Commun. 18 (2001) 1862–1863.
[48] K. Seddon, C. Hardacre, B. Mcauley, Patent, PCT Int. Appl., 2003.
[49] J. Ross, J. Xiao, Green Chem. 4 (2002) 129–133.
[50] S. Nara, J. Harjani, M. Salunkhe, J. Org. Chem. 66 (2001) 8616–8620.
[51] T. Sutto, P. Trulove, H. De Long, Proc.—Electrochem. Soc. 2002-19 (2002) 54–62.
[52] C. Brazel, M. Benton, Abstracts of Papers, 224th ACS National Meeting, Boston, MA, United States, August 18–22, 2002.
[53] M. Benton, C. Brazel, Polymer Preprints, American Chemical Society, Division of Polymer Chemistry 43 (2002) 881–882.
[54] The crystal structure of compound 1 was previously determined using the powder diffraction based structure determination from microcrystalline powder [41]. However, the single crystal was obtained later on and the new results were included into this study as part of the series of presented type of aromatic quaternary ammonium bromides. From structural point of view the powder structure and single crystal structure are analogous.
[55] A.J.M. Duisenberg, L.M.J. Kroon-Batenburg, A.M.M. Schreurs, J. Appl. Crystallogr. 36 (2003) 220–229.
[56] M.C. Burla, M. Camalli, B. Carrozzini, G.L. Cascarano, C. Giacovazzo, G. Polidori, R. Spagna, Sir2002: a new direct methods program for automatic solution and refinement of crystal structures, J. Appl. Crystallogr. 36 (2003) 1103.
[57] G.M. Sheldrick, SHELXS-97, Acta Crystallogr. A 46 (1990) 467–473.
[58] G.M. Sheldrick, SHELXL-97—A Program for Crystal Structure Refinement, University of Gottingen, Germany, 1997.
[59] K. Branderburg, DIAMOND, v 2.1e, Crystal Impact GbR Bonn, Germany, 2000.
[60] E.A. Meyer, R.K. Castellano, F. Diederich, Angew. Chem. Int. Ed. 42 (2003) 1210–1250.
[61] T. Steiner, Angew. Chem. Int. Ed. 41 (2002) 48–76.
[62] CRYSTALLOGRAPHICA software package, J. Appl. Crystallogr. 30 (1997) 418–419.
[63] M. Nissinen, K. Rissanen, Supramol. Chem. (2003) 581–591.